19th Brazilian Congress of Thermal Sciences and Engineering
November 6th–10th, 2022, Bento Gonçalves - RS - Brazil

ENCIT2022-0135
NUMERICAL ANALYSIS OF VOLUMETRIC INEFFICIENCIES OF A SMALL VARIABLE CAPACITY RECIPROCATING COMPRESSOR

Willian T. F. D. Silva
Alessandro S. Pereira
Renatto M. Yupa-Villanueva
Cesar J. Deschamps
POLO Research Laboratories for Emerging Technologies in Cooling and Thermophysics
Federal University of Santa Catarina
Florianópolis – Brazil
willian.duarte@polo.ufsc.br; alessandro.pereira@polo.ufsc.br; renatto.villanueva@polo.ufsc.br; deschamps@polo.ufsc.br

Abstract. *Simulation models are of paramount importance in the design of highly reliable and efficient compressors. This manuscript reports a simulation model to predict the volumetric efficiency of a variable-capacity reciprocating compressor adopted in household refrigeration systems for ASHRAE LBP and ASHRAE MBP operating conditions from 1800 to 6300 rpm. In addition to that, a recently proposed method is used to quantify the main sources of volumetric inefficiencies, including the effects of suction gas superheating, suction process, supercharging/backflow, re-expansion, leakage through the piston-cylinder, irreversibility during re-expansion and valve closure delay. After being validated through comparisons with experimental data, the model was used to analyze the compressor performance under different operating conditions to identify the most critical parameters regarding the volumetric efficiency. The results have shown a nonlinear variation for the volumetric efficiency with the compressor speed under both operating conditions. Additionally, we found that all the inefficiencies for the LBP operating conditions are greater compared to those of the MBP operating conditions for all compressor speed interval. Finally, an increase in compressor speed was found to significantly increase inefficiencies associated with suction gas superheating, suction process, and discharge valve closure delay.*

Keywords: *simulation, variable-capacity, reciprocating compressors, volumetric efficiency*

1. INTRODUCTION

Reciprocating compressors are responsible to promote the flow of the refrigerant fluid in refrigeration systems and, together with the expansion device, establishing the required saturation pressures in the evaporator and condenser. Compressors are generally designed to work under a fixed rotational speed, but the performance of refrigeration systems can be increased if a variable-capacity compressor is used instead (Wang *et al.*, 2015), allowing a better match between the refrigeration demand and the supplied cooling capacity of the compressor. However, the compressor performance should be assessed at different rotational speeds, and the detachment of its inefficiencies may be useful for in-depth analysis.

Pérez-Segarra *et al.* (2005) presented a method to detach volumetric inefficiencies, considering motor slip, clearance volume, suction process, backflow, and leakage in the piston-cylinder gap. Nevertheless, their method disregarded relevant terms such as suction gas superheating. Schreiner *et al.* (2010) improved the method proposed by Pérez-Segarra *et al.* (2005), with the inclusion of terms to quantify inefficiencies related to suction gas superheating, opening delay of the suction valve, and other phenomena during the re-expansion process. However, some terms were found difficult to implement in numerical models used to simulate reciprocating compressors. Santos and Deschamps (2020) developed a method based on the works of Pérez-Segarra *et al.* (2005) and Schreiner *et al.* (2010), including terms due to the suction process and irreversibility during re-expansion. The authors showed that the compressor rotational speed affects the volumetric efficiency due to variations in the suction gas superheating and valve backflow. However, only two rotational speeds were evaluated, which hindered the volumetric inefficiency analysis of the variable-capacity reciprocating compressors.

This paper presents an analysis of the volumetric inefficiencies of a small variable-capacity compressor under different rotational speeds for two operating conditions applying the method proposed by Santos and Deschamps (2020).

2. COMPUTATIONAL MODEL

The computational model adopted to simulate the variable-capacity reciprocating compressor comprises: (i) compression cycle model and (ii) thermal model. On the other hand, bearings are not modeled, and the electric motor was characterized through a curve of the motor efficiency as a function of the compressor rotational speed. The models were implemented in the commercial code GT-SUITE™ and solved in a coupled way as seen in Fig. 1. The details and solution procedure for each model are explained in the following sections.

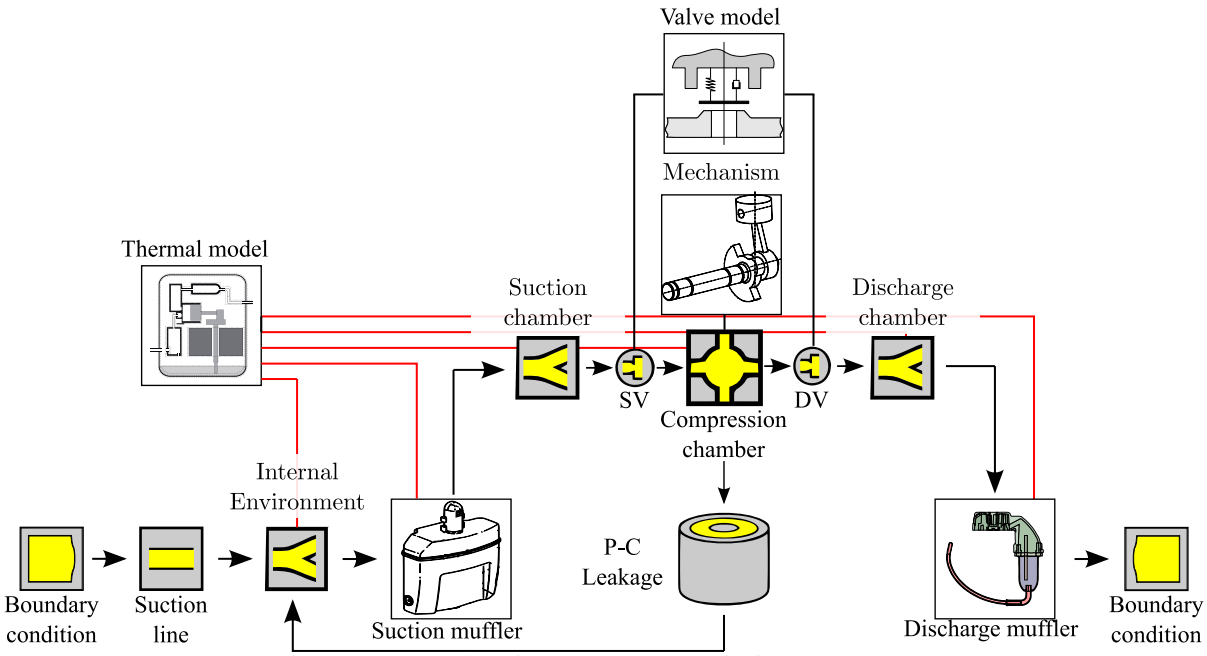

Figure 1: Comprehensive compressor model in GT-SUITE™.

2.1 Compression cycle model

The compression cycle model consists of groups of mathematical expressions that describe three of the compressor components: (i) compressor chamber, (ii) valves, and (iii) mufflers.

The time-dependent volume of the compression chamber is evaluated from expressions of the piston motion. The conservation equations of mass and energy allow the determination of pressure and temperature inside the compression chamber. The fluid flow in the clearance between the piston and the cylinder is modeled as one-dimensional and compressible (Nicoluzzi *et al.*, 2020).

The valve dynamics are modeled as a one-degree-of-freedom system, with the stiffness being obtained via the finite element method and the damping coefficient being adjusted concerning experimental data of valve motion. The flow-induced pressure load on the valve was calculated through the concept of effective force area, obtained via three-dimensional numerical simulations. The mass flow rates through the suction and discharge orifices were calculated using the effective flow area concerning a one-dimensional isentropic flow in a convergent nozzle, but incorporating viscous friction effects.

The compressible fluid flow in the suction and discharge mufflers and their chambers was modeled as tubes and volumes following a one-dimensional approach. Fluid flow was solved with the finite-volume method (Link and Deschamps, 2011) and a time-explicit scheme. The fluid properties at each time step were obtained from the REFPROP library (Lemmon *et al.*, 2018).

2.2 Thermal model

A thermal model is used to calculate the temperature distribution in the compressor. Control volumes with uniform temperature were considered for the compression chamber, suction and discharge mufflers, discharge tube, oil, electric motor, shell, and internal environment (Diniz *et al.*, 2019). Thermal conductances calibrated by temperature measurements in different regions inside the compressor were used to estimate the heat transfer between the control volumes. The thermal conductances were adjusted as a function of the compressor rotational speed. Moreover, heat generation due to viscous friction in bearings and electrical motor inefficiency were specified as a function of the rotational speed and included as source terms in the equations.

2.3 Solution procedure

The equations of the compression cycle model and the thermal model were solved by employing a fifth-order Runge-Kutta method in a coupled way using an unsteady formulation with an explicit time integration scheme. The time step size was calculated by establishing the Courant–Friedrichs–Lewy criterion smaller than 0.7 to ensure the numerical stability of the solution procedure. The boundary conditions adopted in the simulation model were the evaporating and condensing temperatures and the temperature of the external environment. The initial conditions for the temperature and pressure in the compression chamber and suction muffler were prescribed as those of the evaporating condition, while the condensing condition was used to prescribe the pressure and temperature for the discharge line. The solution procedure was considered to have converged when differences of less than 0.2% for pressure and mass flow rate and less than 0.1K for temperature were found between two consecutive compression cycles.

3. METHODOLOGY

The methodology used in this investigation consisted of (i) determining the volumetric efficiency and (ii) detaching it in terms of inefficiencies, following the method proposed by Santos and Deschamps (2020). The volumetric efficiency of a compressor is defined as the ratio between the actual mass flow rate, $\dot{m}$, and the theoretical mass flow rate, $\dot{m}_{\mathrm{th}}$.

The theoretical mass flow rate corresponds to an ideal compressor with the following characteristics: (i) no heat transfer or pressure drop in the suction path, (ii) isobaric conditions during the admission and discharge processes and no backflow, (iii) absence of leakage in the compression chamber, (iv) no-slip condition in the electric motor and (v) no clearance volume. The mass flow rate of an ideal compressor can be obtained from

$$\dot{m}_{\mathrm{th}} = f\ \rho_{\mathrm{sl}}\ V_{\mathrm{sw}} \tag{1}$$

where f represents the nominal operating frequency of the motor, ρ_{sl} is the density at the suction line, and V_{sw} is the total volume swept by the piston.

Therefore, the volumetric efficiency η_{v} is

$$\eta_{\mathrm{v}} = \frac{\dot{m}}{\dot{m}_{\mathrm{th}}} = \frac{\dot{m}_{\mathrm{th}} - \Delta\dot{m}_{\mathrm{total}}}{\dot{m}_{\mathrm{th}}} \tag{2}$$

where the actual mass flow rate can be written as the theoretical mass flow rate minus the total mass flow reduction, $\Delta\dot{m}_{total}$, brought about by different inefficiencies.

The detachment of the volumetric inefficiencies consists in splitting the total reduction of the mass flow rate into contributions of different sub-processes, i.e.

$$\Delta\dot{m}_{\mathrm{total}} = \sum_{i} \Delta\dot{m}_{\mathrm{i}} \tag{3}$$

The sub-index i indicates a local source of inefficiency. Additionally, these local mass flow reductions can be expressed in terms of local volumetric inefficiencies $\Delta\eta_{v_i}$, by introducing replacing Eq. (3) in Eq. (2), resulting in Eq. (4):

$$\eta_{\mathrm{v}} = 1 - \sum_{i} \Delta\eta_{\mathrm{v_i}}. \tag{4}$$

Figure 2 shows the $p-V$ diagram of the compression cycle used to identify volumetric inefficiencies. Point C denotes the thermodynamic state in which the pressure in the compression chamber reaches the discharge pressure, p_{dis}. Point C' represents the thermodynamic state that would be reached after an ideal isobaric discharge from C to the top dead center (TDC). The end of the actual discharge process could take place after the TDC, point D, with possible backflow in the discharge valve. The re-expansion process occurs after the point D, followed by the suction process that can extend up to the point B, beyond the bottom dead center (BDC). The points a_1 and a_2 designate the thermodynamic states of the gas after the isentropic expansion from the states C and D to suction pressure, p_{suc}, respectively. Finally, the point a stands for the thermodynamic state reached after the real expansion process from state D, including therefore leakage, heat transfer and non-ideality of the gas.

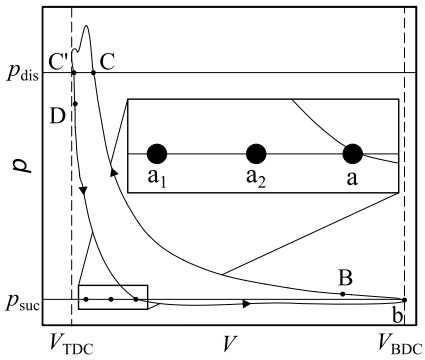

Figure 2: Schematics of an actual $p-V$ diagram indicating the points used to compute the local volumetric inefficiencies.

The equations in Tab. 1 characterize the inefficiencies associated with the phenomena that occur as the gas flows from the suction path (i) through the compression chamber (ii) to the discharge chamber (iii). In this table, the densities of the gas at the suction line and suction chamber are denoted by ρ_{sl} and ρ_{sc}, respectively. The mass flow rates through the suction and discharge orifices are $\dot{m}_{\mathrm{suc}}$ and $\dot{m}_{\mathrm{dis}}$, respectively. The mass flow rate in the clearance between the piston and the cylinder is denoted as $\dot{m}_{\mathrm{leak}}$. The volume swept by the piston inside the cylinder is V_{sw}.

Table 1: Equations to estimate inefficiencies classified by the gas path.

Gas path	**Inefficiency**	$\boldsymbol{\Delta}\eta_{\mathrm{v_i}}$
Suction	Superheating	$(\rho_{\mathrm{sl}}-\rho_{\mathrm{sc}})\,V_{\mathrm{sw}}/\rho_{\mathrm{sl}}V_{\mathrm{sw}}$
	Suction supercharging and backflow	$\left(\int_b^B \dot{m}_{\mathrm{suc}}dt\right)/\rho_{\mathrm{sl}}V_{\mathrm{sw}}$
	Suction process	$(\rho_{\mathrm{sc}}V_{\mathrm{ab}}-\int_a^b \dot{m}_{\mathrm{suc}}\,dt)/\rho_1 V_{\mathrm{sw}}$
Compression chamber	Re-expansion process	$\rho_{\mathrm{sc}}\,(V_{\mathrm{sw}}-V_{\mathrm{a_1b}})\,/\rho_{\mathrm{sl}}V_{\mathrm{sw}}$
	Irreversibility during re-expansion	$\rho_{\mathrm{sc}}\,(V_{a_1b}-V_{a_2b})\,/\rho_{\mathrm{sl}}V_{\mathrm{sw}}$
	Leakage through piston-cylinder clerance	$m_{leak}/\rho_{\mathrm{sl}}V_{\mathrm{sw}}$
Discharge	Discharge valve closure delay	$\rho_{\mathrm{sc}}\,(V_{\mathrm{a_2}}-V_{\mathrm{a_3b}})\,/\rho_{\mathrm{sl}}V_{\mathrm{sw}}$

4. RESULTS

Two operating conditions were selected for the present analysis, ASHRAE LBP ($T_{\mathrm{v}}=-23.3\ ^o\mathrm{C}$; $T_{\mathrm{c}}=54.4\ ^o\mathrm{C}$) and ASHRAE MBP ($T_{\mathrm{v}}=-6.7\ ^o\mathrm{C}$; $T_{\mathrm{c}}=54.4\ ^o\mathrm{C}$), under 19 rotational speeds in the range of 1800 rpm to 6300 rpm. The refrigerant R600a was adopted as the working fluid.

4.1 Validation of the numerical model

The simulation model was validated via comparisons between predictions and experimental data. Initially, a p-V diagram for the ASHRAE LBP operating condition and rotational speed of 2800 rpm was selected, followed by results of mass flow rates for speeds of 1800, 2800, 4000, and 6300 rpm.

Numerical and experimental results for the $p-V$ diagram in Fig. 3 show excellent agreement during the compression and expansion processes, Fig. 3a, and a small difference in the suction and discharge processes. During the suction process, the highest difference is around 0.04 bar at $V/V_{\max}=0.6$, as shown in Fig. 3b. As for the discharge process, there is a maximum difference of 0.3 bar at $V/V_{\max}=0.06$, as shown in Fig. 3c. Despite these minor differences, the model is considered suitable to predict the pressure inside the cylinder in the presence of all the processes (suction gas superheating, suction process, re-expansion process, leakage, heat transfer, etc.).

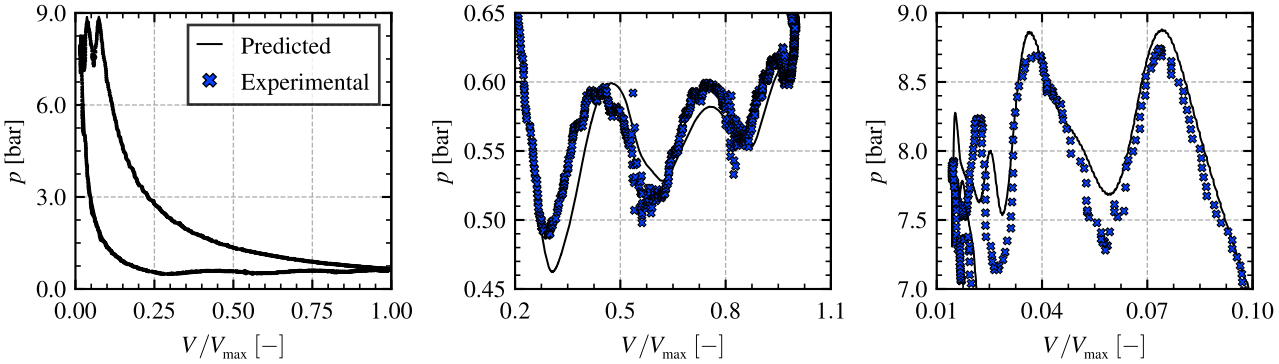

(a) Entire cycle (b) Suction process (c) Discharge process

Figure 3: Predictions and experimental results for the $p - V$ diagram: LBP condition and 2800 rpm.

The numerical and experimental results of mass flow rates for the LBP condition, considering four rotational speeds, are presented in Fig. 4. The results are given in the dimensionless form, with the mass flow rate divided by the experimental mass flow rate at 6300 rpm. Differences of 3.8%, 0.5%, 3.2%, and 3.5% were obtained for 1800, 2800, 4000, and 6300 rpm, respectively. Therefore, a good agreement was again observed between the predictions and the experimental data, indicating that the simulation model can also predict mass flow rates under different rotational speeds.

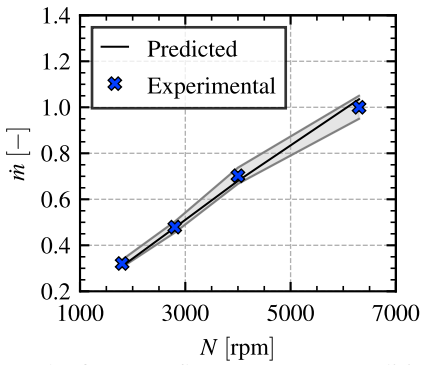

Figure 4: Predictions and experimental results for mass flow rate: LBP condition and 1800, 2300, 3300, and 6300 rpm.

4.2 Volumetric efficiency

The predicted volumetric efficiencies under different rotational speeds for LBP and MBP conditions are shown in Fig. 5. Regarding the LBP condition, the high efficiencies of 71.0%, 70.8%, 72.5% and 70.2% are observed for 1800, 2500, 3300, and 4800 rpm, respectively. As expected, the volumetric efficiencies for the MBP condition are greater than those of the LBP condition for all rotational speeds obtained, with values of 82.0%, 81.8%, and 82.0% found for 2300, 3000, 3500, respectively. Interestingly, the variation of the volumetric efficiency is not a monotonic function of the compressor speed. In fact, a wavy pattern is observed for volumetric efficiency under LBP and MBP conditions, mainly for speeds less than 5000 rpm. This pattern was also reported by Nagata *et al.* (2010) and Tao *et al.* (2018). As will be seen shortly, the detachment of volumetric inefficiencies is a suitable strategy to explain these features.

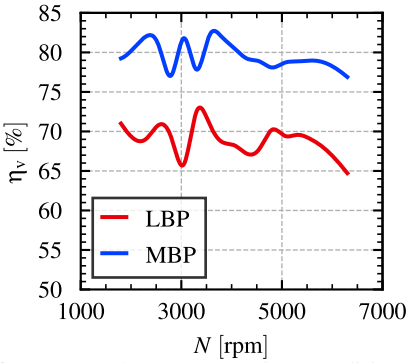

Figure 5: Volumetric efficiency for LBP and MBP operating conditions under several rotational speeds.

4.3 Detachment of inefficiencies

The volumetric inefficiencies associated with the suction path can be separated into suction gas superheating, suction process, and supercharging/backflow, as shown in Fig. 6. Regarding the superheating of suction gas, Fig. 6a shows that the inefficiencies for the LBP condition increase with the compressor speed and are greater than those for the MBP condition for all rotational speeds. For the LBP condition, the minimum and maximum inefficiencies of 6.3% were found for 1800 rpm and 12.9% for 6300 rpm, respectively, while for the MBP the minimum and maximum inefficiencies of 5.6% and 11.9% were predicted for the same rotational speeds.

The inefficiencies related to the suction process are shown in Fig. 6b. As can be seen, the inefficiencies are higher for the LBP condition when compared with the MBP condition. It can be noted that the inefficiencies seem to be insensitive to changes of the rotational speed up to approximately 4000 rpm (LBP) and 5000 rpm (MBP), but there is a considerable increase at higher speeds. For the LBP condition the maximum inefficiency corresponds to 9.6% at 5500 rpm, while for the MBP condition, the maximum inefficiency of 8.9% was found under 6300 rpm.

The volumetric inefficiencies due to supercharging/backflow are shown in Fig. 6c. It should be noted that the inefficiency is negligible under 3000 rpm under both conditions (MBP and LBP). As the rotational speed increases to more than 3000 rpm, this inefficiency presents only negative values for both conditions (except at LBP in 4800 rpm), indicating an increase in the mass flow rate. This phenomenon of suction supercharging was also reported by Liu (1993). For instance, a maximum increase of 5.9% in the mass flow rate is predicted for the compressor operating under the LBP condition working and 5300 rpm, whereas a similar increase is also observed for the MBP condition, but with a speed of 6300 rpm.

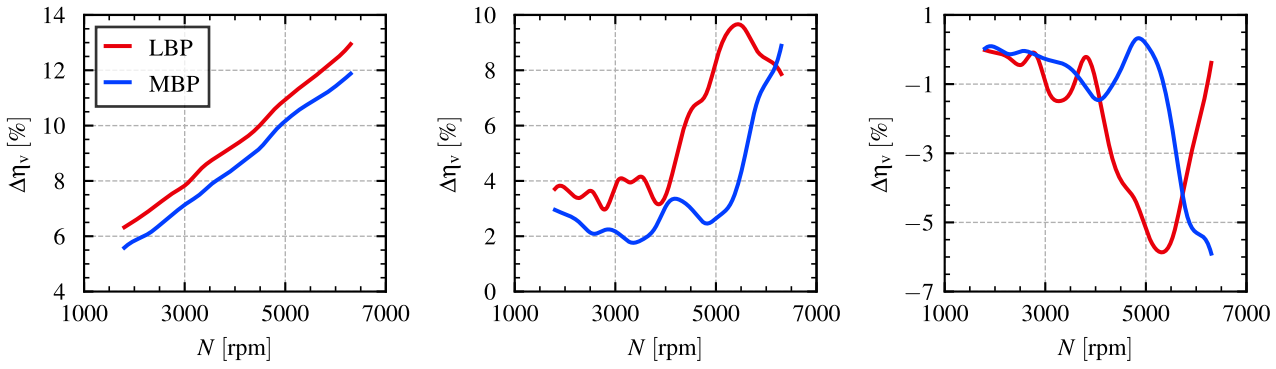

(a) Suction gas superheating (b) Suction process (c) Supercharging/backflow

Figure 6: Volumetric inefficiencies in the suction path for LBP and MBP operating conditions under several rotational speeds.

The volumetric inefficiencies associated with the compression chamber are split into the re-expansion process, leakage through the piston-cylinder (P-C) gap, and non-ideality of the re-expansion process. Regarding re-expansion, Fig. 7a shows a decrease in the inefficiency for both conditions as the rotational speed increases, with the highest values being observed for the LBP condition due to its higher pressure ratio compared with the MBP condition. Hence the residual gas in the compression chamber has to be expanded from discharge pressure to a lower suction pressure before the suction valve can open. Therefore, since the pressure ratio for the LBP condition is greater than that of the MBP condition, this suction process is delayed, decreasing volumetric efficiency. The maximum inefficiencies were predicted for the compressor running under 1800 rpm, reaching 14.7% and 7.2% for the LBP and MBP operating conditions.

Figure 7b shows the volumetric inefficiencies associated with the leakage through the piston-cylinder clearance (P-C leakage). The greatest inefficiencies occur at low speeds, as also observed by Liu (1993) and Krueger and Schwarz (1994), reaching 4.6% and 3.5% for both operating conditions under 1800 rpm. Concerning the inefficiency associated with the non-ideality of the re-expansion process, the results show negligible negative values in all rotational speed intervals, as presented in Fig. 7c.

The delay of the discharge valve closure gives rise to backflow, which reduces the volumetric efficiency as seen in Fig. 8. Compared to the other inefficiencies already discussed, this inefficiency has more oscillations as the rotational speed is varied for the LBP and MBP operating conditions, specially in low to medium compressor speed range, where more valve fluttering is found. Nagata *et al.* (2010) and Tao *et al.* (2018) found similar oscillations when exploring the effect of backflow in the suction valve. For the LBP condition, the maximum inefficiency is observed at 3000 rpm, while for the MBP the maximum inefficiency occurs at 3300 rpm. In general, this inefficiency is found to be more critical for the LBP condition. The oscillations of this inefficiency can explain the wavy pattern of the volumetric efficiency shown in Fig. 5.

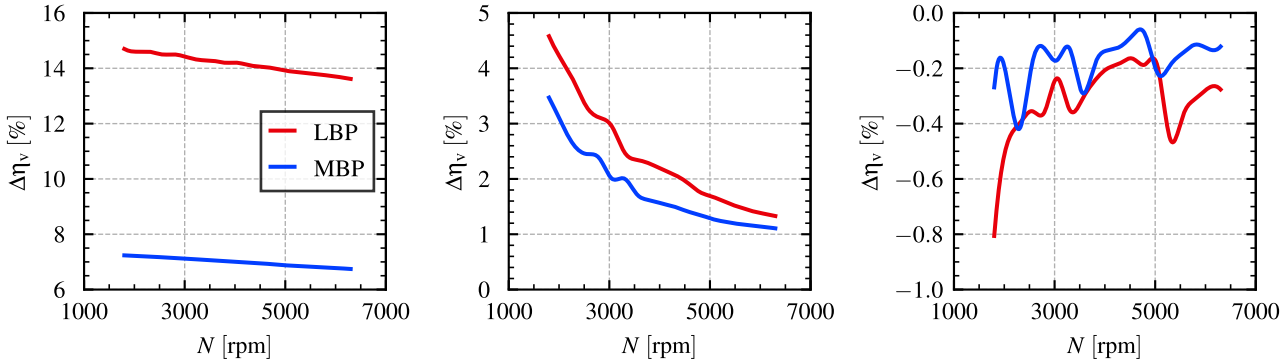

(a) Re-expansion process (b) P-C leakage (c) Non-ideality of re-expansion process

Figure 7: Volumetric inefficiencies at the compression chamber for LBP and MBP operating conditions under several rotational speeds.

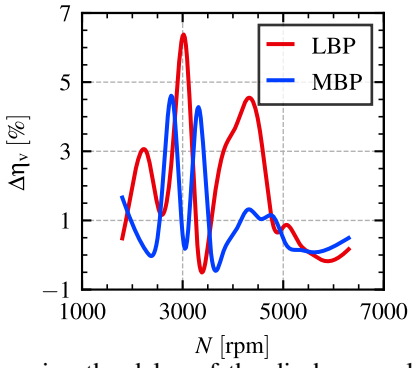

Figure 8: Volumetric inefficiencies concerning the delay of the discharge valve closure for LBP and MBP operating conditions under several rotational speeds.

5. CONCLUSIONS

The detachment of the volumetric inefficiencies is required for the optimization of compressors. In this paper, a variable-capacity compressor used for refrigeration was numerically analyzed under nineteen rotational speeds ranging from 1800 rpm and 6300 rpm under the ASHRAE LBP and ASHRAE MBP operations conditions. After being validated through comparisons with experimental data, predictions of volumetric efficiencies showed a wavy pattern for both conditions, mainly for rotational speeds lower than 5000 rpm. A recent method proposed to detach volumetric inefficiencies following the gas path (suction, compression chamber, and discharge) was adopted to analyze the main factors affecting compressor volumetric efficiency. Concerning the suction path, three sources of inefficiency were considered: (i) suction gas superheating, (ii) suction process, and (iii) supercharging/backflow. The suction gas superheating and suction process were more critical for the LBP condition than for the MBP condition. The supercharging/backflow presented negative inefficiencies values, indicating the increase of the mass flow rate due to supercharging. Regarding the compressor chamber, the inefficiencies were analyzed in three aspects: (i) re-expansion process, (ii) leakage through the piston-cylinder clearance, and (iii) non-ideality of the re-expansion process. As expected, the re-expansion process is quite critical in the LBP condition, being the primary reason for the lower volumetric efficiency in comparison with the MBP condition. Leakage through the piston-cylinder clearance also presented higher values for the LBP conditions compared to the MBP condition, being more critical under low rotational speeds. Finally, the inefficiency brought about by the delay of the discharge valve closure was explored regarding the discharge path. This inefficiency was critical for the compressor operating under the LBP condition at 3000 rpm, reducing up to 6.5% the compressor capacity. This inefficiency presents an oscillatory pattern with the compressor speed, which can explain the oscillations found in the volumetric efficiency when the compressor speed is varied. Overall, the method adopted to detach volumetric inefficiencies was shown to be valuable in the optimization of variable-capacity compressors, allowing identification and quantification of the main sources of inefficiencies.

6. ACKNOWLEDGEMENTS

The authors appreciate the support from Nidec-GA and EMBRAPII (“Development of new technologies for refrigeration compressors” Project). Additional funding was provided by the National Institutes of Science and Technology

(INCT) Program (CNPq Grant No. 404023/2019-3; FAPESC Grant No. 2019TR0846) and CAPES (Coordination for the Improvement of Higher Education Personnel).

7. REFERENCES

Diniz, M.C., Hermes, C.J. and Deschamps, C.J., 2019. "Transient simulation of small-capacity reciprocating compressors in on-off controlled refrigerators". *Int. J. Refrigeration*, Vol. 102, pp. 12–21. doi:https://doi.org/10.1016/j.ijrefrig.2019.03.005.

Krueger, M. and Schwarz, M., 1994. "Experimental analysis of a variable-speed compressor". In *Proc. Int. Compressor Engineering Conference at Purdue*. URL `https://docs.lib.purdue.edu/icec/1042/`.

Lemmon, E.W., Bell, I.H., Huber, M.L. and McLinden, M.O., 2018. "Nist standard reference database 23: Reference fluid thermodynamic and transport properties-refprop, version 10.0, national institute of standards and technology". *Standard Reference Data Program, Gaithersburg*.

Link, R. and Deschamps, C.J., 2011. "Numerical modeling of startup and shutdown transients in reciprocating compressors". *Int. J. Refrigeration*, Vol. 34, No. 6, pp. 1398–1414. doi:https://doi.org/10.1016/j.ijrefrig.2011.04.005.

Liu, Z., 1993. *Simulation of a Variable Speed Compressor with Special Attention to Supercharging Effects*. Ph.D. thesis.

Nagata, S., Nozaki, T. and Akizawa, T., 2010. "Analysis of dynamic behavior of suction valve using strain gauge in reciprocating compressor". In *Proc. Int. Compressor Engineering Conference at Purdue*. URL `https://docs.lib.purdue.edu/icec/1979/`.

Nicoluzzi, M., Braga, V.M. and Deschamps, C.J., 2020. "Predicting leakage of refrigerant in the piston cylinder clearance of reciprocating compressors". In *Proceedings of the 18th Brazilian Congress of Thermal Sciences and Engineering - ENCIT 2020*. doi:https://doi.org/10.26678/ABCM.ENCIT2020.CIT20-0261.

Pérez-Segarra, C.D., Rigola, J., Sòria, M. and Oliva, A., 2005. "Detailed thermodynamic characterization of hermetic reciprocating compressors". *Int. J. Refrigeration*, Vol. 28, pp. 579–593. doi:10.1016/j.ijrefrig.2004.09.014.

Santos, L.M. and Deschamps, C.J., 2020. "Characterization of volumetric inefficiencies of reciprocating compressors adopted in small capacity refrigeration systems". In *Proceedings of the 18th Brazilian Congress of Thermal Sciences and Engineering - ENCIT 2020*. doi:https://doi.org/10.26678/ABCM.ENCIT2020.CIT20-0280.

Schreiner, J.E., Deschamps, C.J. and Barbosa, J.R., 2010. "Theoretical analysis of the volumetric efficiency reduction in reciprocating compressors due to in-cylinder thermodynamics". In *Proc. Int. Compressor Engineering Conference at Purdue*. URL `https://docs.lib.purdue.edu/icec/2004`.

Tao, W., Guo, Y., He, Z. and Peng, X., 2018. "Investigation on the delayed closure of the suction valve in the refrigerator compressor by fsi modeling". *Int. J. Refrigeration*, Vol. 91, pp. 111–121. doi:https://doi.org/10.1016/j.ijrefrig.2018.05.004.

Wang, L., Liu, G.B., Zhao, Y.Y. and Li, L.L., 2015. "Performance comparison of capacity control methods for reciprocating compressors". In *Proc. 9th Int. Conf. on Compressors and their Systems*. IOP Conference Series: Materials Science and Engineering, Vol. 90. doi::10.1088/1757-899X/90/1/01202.

8. RESPONSIBILITY NOTICE

The authors are the only ones responsible for the printed material included in this paper.